

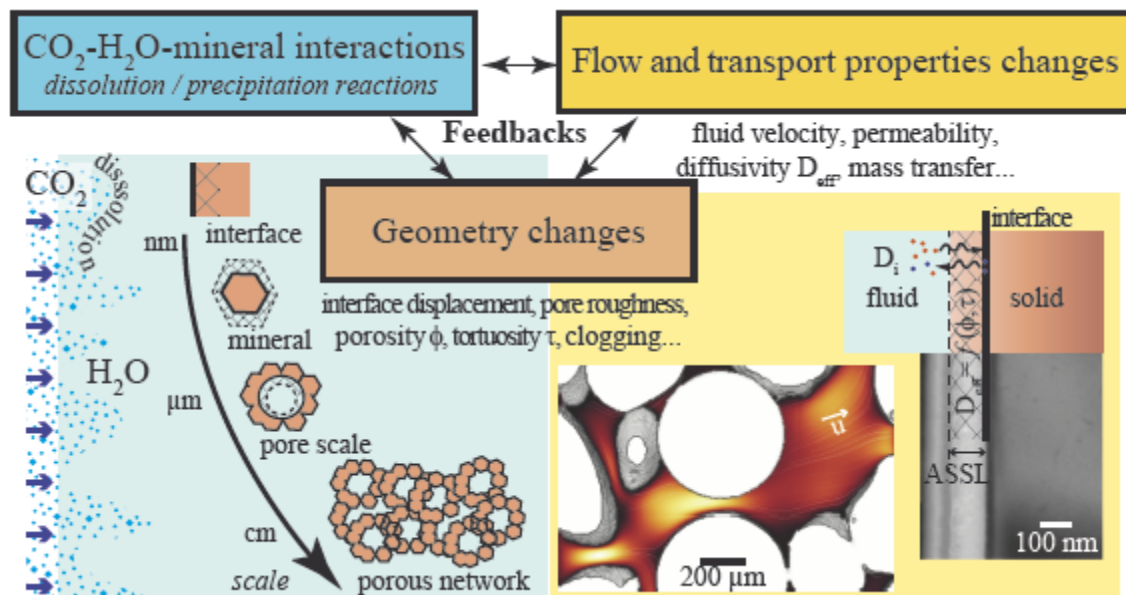
Pore-scale geochemical reactivity associated with CO₂ storage: new frontiers at the fluid-solid interface.

Catherine Noiriel^{*,1} and Damien Daval²

¹Géosciences Environnement Toulouse, Observatoire Midi-Pyrénées, Université Paul Sabatier, CNRS, IRD, 14 avenue Edouard Belin, F-31400 Toulouse, France. catherine.noiriel@univ-tlse3.fr

²Laboratoire d'Hydrologie et de Géochimie de Strasbourg, Université de Strasbourg, EOST, CNRS, 67084 Strasbourg, France. ddaval@unistra.fr

CONSPECTUS



The reactivity of carbonate and silicate minerals is at the heart of porosity and pore geometry changes in rocks injected with CO₂, which ultimately control the evolution of flow and transport properties of fluids in porous and/or fractured geological reservoirs. Modeling the dynamics of CO₂-water-rock interactions is challenging due to the resulting large geochemical disequilibrium, the reservoir heterogeneities, and the large space and time scales involved in the processes. In particular, there is a lack of information about how the macroscopic properties of a reservoir, e.g., the permeability, will evolve as a result of geochemical reactions at the molecular scale. Addressing this point requires a fundamental understanding of how the microstructures influence the macroscopic properties of rocks. The pore scale, which ranges from a few nm to cm, has stood out as an essential scale of observation of geochemical processes in rocks. Transport or surface reactivity limitations due to the pore space architecture, for instance, are best described at the pore scale itself. It can be also considered as a meso-scale for aggregating and increasing the gain of fundamental understanding of microscopic interfacial processes. Here, we focus on the

potential application of a combination of physico-chemical measurements coupled with nanoscale and microscale imaging techniques during laboratory experiments to improve our understanding of the physico-chemical mechanisms that occur at the fluid-solid interface, and the dynamics of the coupling between the geochemical reactions and flow and transport modifications at the pore scale. Imaging techniques, such as atomic force microscopy (AFM), vertical scanning interferometry (VSI), focused ion beam-transmission electron microscopy (FIB-TEM) and X-ray microtomography (XMT), are ideal for investigating the reactivity dynamics of these complex materials.

Minerals and mineral assemblages, i.e., rocks, exhibit heterogeneous and anisotropic reactivity, which challenges the continuum description of porous media and assumptions required for reactive transport modeling at larger scales. The conventional approach, which consists of developing dissolution rate laws normalized to the surface area, should be revisited to account for both the anisotropic crystallographic structure of minerals and the transport of chemical species near the interface, which are responsible for the intrinsic evolution of the mineral dissolution rate as the reaction progresses. In addition, the crystal morphology and the mineral assemblage composition, texture and structural heterogeneities are crucial in determining whether the permeability and transport properties of the reservoir will be altered drastically or maintain the sealing properties required to ensure the safe sequestration of CO₂ for hundreds of years. Investigating the transport properties in nm- to μm-thick amorphous Si-rich surface layers (ASSLs), which develop at the fluid-mineral interface in silicates, provides future direction, as ASSLs may prevent contact between the dissolving solids and the pore fluid, potentially inhibiting the dissolution/carbonation process. Equally, at a larger scale, the growth of μm- to mm-thick alteration layers which result from the difference in reactivity between silicates and

carbonates, slows the transport in the vicinity of the fluid-solid interface in polymineralic rocks, thus limiting the global reactivity of the carbonate matrix. In contrast, in pure limestone, the global reactivity of the monomineralic rock decreases because the flow localization promotes the local reactivity within the forming channels, thus enhancing permeability changes compared to more homogeneous dissolution of the rock matrix.

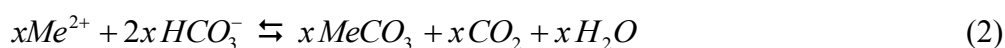
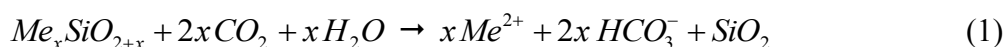
These results indicate that the transformation of the rock matrix should control the evolution of the transport properties in reservoirs injected with CO₂ the same amount as the intrinsic chemical reactivity of the minerals and the reservoir hydrodynamics. This process, which is currently not captured by large-scale modeling of reactive transport, should benefit from the increasing capabilities of non-invasive and non-destructive characterization tools for pore-scale processes, ultimately constraining reactive transport modeling and improving the reliability of predictions.

1. INTRODUCTION

The geologic sequestration of CO₂ through underground injection is an appealing strategy because of the expected long residence time of carbon prior to its putative escape into the atmosphere. The injection of CO₂ in geological reservoirs, e.g. in sedimentary or basalt formations, involves strong geochemical disequilibrium spanning multiple space and time scales. Over short timescales (10-10² years), most of the injected CO₂ is physically stored either as a liquid or in the supercritical phase in the reservoir or dissolved in formation waters¹. However, the increasing proportion of CO₂ sequestered as carbonate minerals over time ultimately controls the long-term storage security, thus requiring a fundamental understanding of the elementary mechanisms of mineral trapping. In that respect, deciphering the mineral reactivity and the

associated modifications of the physico-chemical properties of rocks is an important question before Carbon Capture and Storage (CCS) operations can be widely proposed as a reliable option for the mitigation of CO₂ emissions in the atmosphere.

While the reactivity of minerals in contact with neat or wet CO_{2(sc)} during plume migration are expected to be null or limited, e.g., by the amount of water adsorbed on the mineral surfaces², the acidification of pore waters by CO₂ dissolution along the plume boundary represents a strong thermodynamic driving force for the dissolution of rock-forming minerals and the precipitation of secondary phases. For instance, in the silicate mineral-CO₂-H₂O system, mineral trapping occurs through both the release of divalent cations during the dissolution of silicates (Eq.1) and the pH increase, which in turn promote the precipitation of carbonates (Eq.2):



The magnitude of the driving force that controls the relative intensities of the chemical fluxes associated with the carbonation reaction (combination of Eq.1 and Eq.2), which ultimately contributes to the carbon storage security, is related to the chemical, physical, and geological parameters, e.g., the fluid composition, temperature, CO₂ partial pressure (P_{CO2}), and reservoir mineralogical composition, as well as the flow and transport properties. In particular, the dissolution/precipitation processes depend strongly on the coupling between the local flow velocity and the concentration distributions, and the fate of CO₂ is intimately related to the interplay between the chemical reactions and the transport of species with the fluid. Of equal importance, these processes also depend on the geometry evolution at different scales ranging from the crystal face^{3,4} to the pore space^{5,6}, where dissolution along mineral boundaries and the difference in reactivity between minerals or the formation of secondary precipitates contribute to

the modification of the flow paths at larger scales (Figure 1). The resulting fluid composition also represents a strong Gibbs free energy gradient in various locations of the reservoir, potentially enhancing the contrasts in mineral reactivity along the flow paths. Such changes ultimately enhance the heterogeneity of distributions of the advective/diffusive zones and flow in the reservoir by gradually widening or clogging pores and channels⁷.

Overall, the bulk properties, such as the average concentrations or variations of the molar volumes resulting from carbonation, are essentially meaningless without consideration of both the time-dependent dynamics and the spatialization of the processes from the atomic scale to the continuum scale. Improving the understanding of the non-linear dynamics of geochemical processes coupled to physical processes such as flow and diffusion at the pore scale has received focused attention in recent years⁸. Methods combining experimental techniques relevant to *in situ* CO₂ storage conditions⁹ with analytical tools to characterize the fluid chemistry, mineral composition, surface properties and 3D geometry of porous media have brought new insights into mineral and rock reactivity that challenge conceptual modeling of reactive transport at the continuum scale^{8,10}. In particular, the application of different techniques for the characterization of the fluid-mineral interface, e.g., AFM, VSI, FIB-TEM, or XMT, is changing our understanding of rock reactivity.

In this Account, we review some of the recent breakthroughs regarding pore-scale geochemical reactivity in connection with the fluid-solid interface. We also discuss how the combined impacts of physical and chemical heterogeneities in minerals and rocks can lead to paradigm shifts in both conventional descriptions of solid reactivity and unexpected, emergent behaviors, whose assessment is among the key issues to better evaluate the fate of CO₂ over large time and spatial scales.

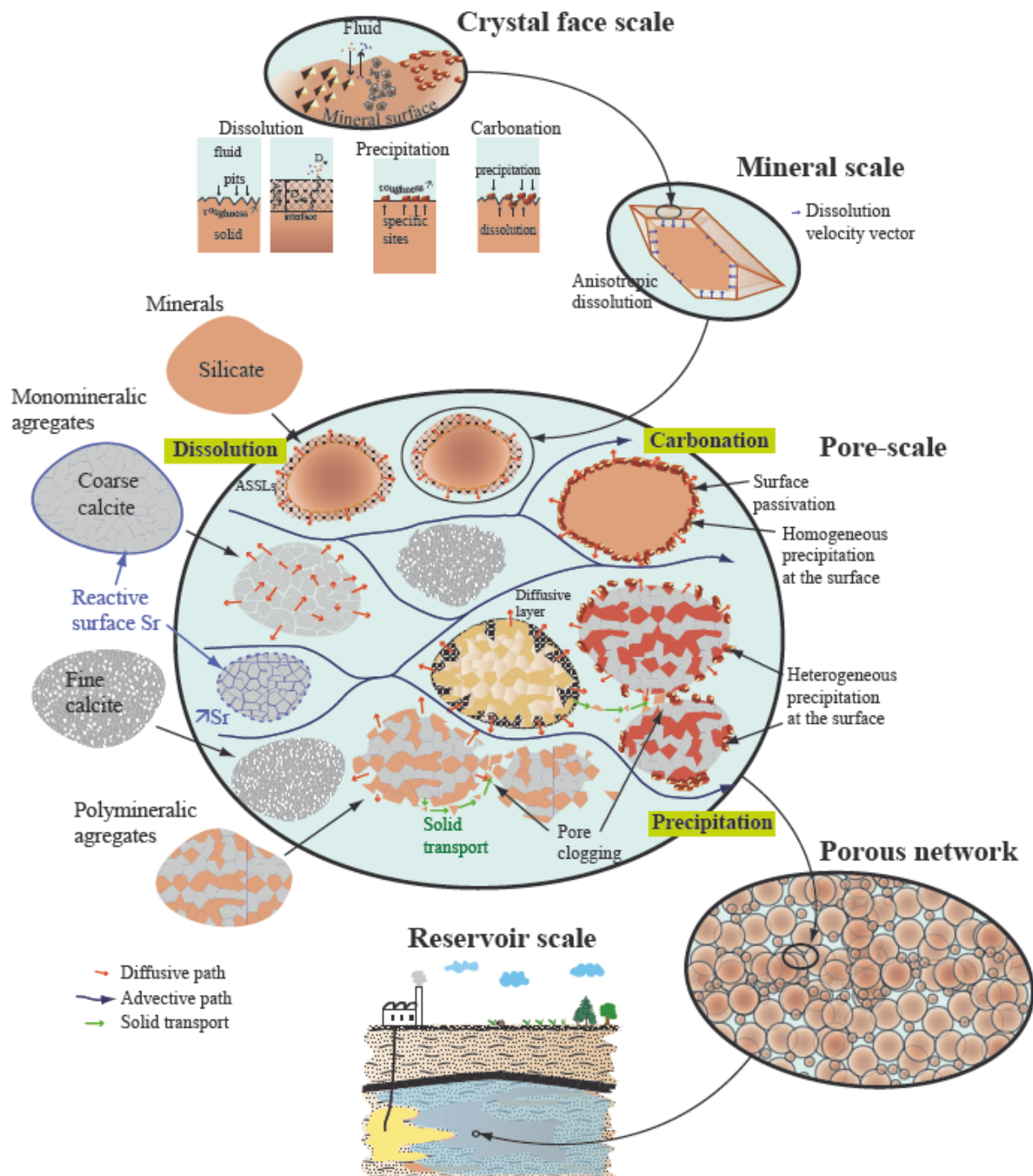


Figure 1. Schematic view of mineral and rock reactivity at the pore scale.

2. MINERAL REACTIVITY: BEYOND THE SURFACE AREA CONCEPT

2.1 Parameterization

The parameterization of mineral dissolution/precipitation kinetics originates from the transposition of transition state theory (TST), which was initially developed for elementary reactions in homogeneous media¹¹, to overall dissolution processes in heterogeneous media. The resulting dissolution/precipitation rate law, which describes surface-controlled reaction kinetics, can be written¹²:

$$r_{\min} = \frac{d\xi}{dt} = \pm k_r S_r \exp\left(-\frac{E_a}{RT}\right) \prod_i [a_i]^{j_i} f(\Delta G(T)) \quad (3)$$

where r_{\min} is the mineral dissolution/precipitation rate [$\text{mol}\cdot\text{s}^{-1}$], ξ is the overall reaction progress, t is the time, k_r is the rate constant [$\text{mol}\cdot\text{m}^{-2}\cdot\text{s}^{-1}$], S_r is the *effective* surface area, E_a is the apparent activation energy, a_i is the activity of aqueous species i and R and T are the gas constant and temperature, respectively. The term $\prod_i [a_i]^{j_i}$ accounts for the inhibiting or promoting effects of aqueous species on the overall reaction, and $f(\Delta G(T))$ is a function accounting for the driving force of the reaction, i.e., the Gibbs free energy, ΔG .

While the applicability of the TST-based formulation has been called into question on several levels⁸, one limitation of Eq. (3) concerns the *effective* surface area, S_r , which is often used as a fitting parameter in modeling exercises. Generally, the reaction rate is normalized with respect to either the geometric surface area calculated from the crystal dimensions while ignoring surface roughness or the BET¹³ surface area determined from gas adsorption. Divergences already exist between these normalization methods, which also precludes any potential dependence of the reaction rate on the crystal habit, the surface aspect ratio or the reaction progress and, thus, the surface evolution. As a matter of fact, the fundamental assumptions hidden behind the normalization methods are (i) homogeneity, (ii) isotropy and (iii) immutability of the mineral

surface. However, mineral dissolution/precipitation reactions do not support any of these concepts, suggesting that the conventional treatment of dissolution/precipitation kinetics may have to be revisited.

2.2. Challenging the homogeneity paradigm

While heterogeneous dissolution of synthetic¹⁴ and natural¹⁵ crystals has been observed and theorized for decades, it has been gradually recognized that silicate dissolution proceeds via etch pit formation at dislocation outcrops (Figure 2a-d), resulting in a substantial increase in the surface area exposed to the fluid. However, the exact role of etch pits in controlling the overall dissolution rate of powdered minerals, as well as the intrinsic reactivity of pit walls has long remained speculative or controversial¹⁶. In particular, the lack of a dependence of the rate on the dislocation density and the observation of steady-state rates despite the continuous formation of etch pits seemed to indicate a modest contribution of the etch pits to the process, which was essentially restricted to the poorly-reactive pit walls^{16,17}. Advances in nanoscale measurements of surface topography coupled to numerical modeling have helped demonstrate that the lack of dependence of the dissolution rate on the dislocation density was due to stepwave annihilation and etch pit coalescence^{4,18}. Equally important, the reactivity of pit walls can either be greater or lower than that of the face on which they develop^{4,19}. More generally, the variability of the surface reactivity of minerals is well illustrated through the heterogeneous distribution of reaction rates at the crystal surface, e.g., calcite²⁰, which reflects the diversity of energetic sites and reaction mechanisms. At a larger scale, 3D measurements using XMT (Figure 2e-i) reveal that spatial variation of the dissolution rate is mostly localized at the crystal edges and corners, whereas the initial coarse heterogeneities at the crystal surface are progressively smoothed.

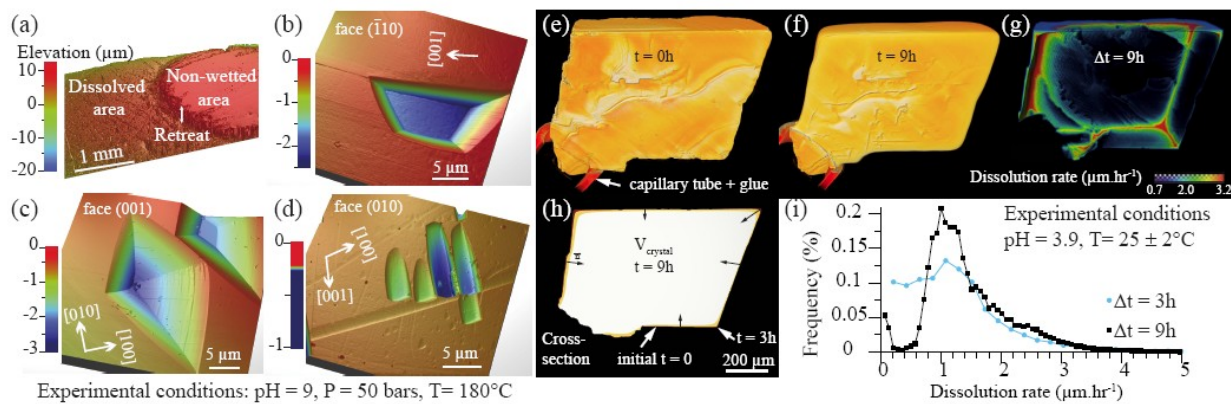


Figure 2. (a) Illustration of surface retreat measurements using VSI, and (b-d) AFM observations of etch pit morphologies developed on various orthoclase faces (see ⁴ for experimental details). (e-f) XMT observations of a calcite crystal during dissolution, (g) analysis of volume changes ($t = 0, 3$ and 9h), and (h-i) corresponding distribution of rates.

2.3. Challenging the isotropy paradigm

The advent of nanoscale imaging of surface topography has also made the comprehensive quantification of dissolution anisotropy and the reexamination of the formalism that describes mineral dissolution possible²¹⁻²⁴. The anisotropic reactivity of minerals originates from the anisotropic distribution of atomic positions in the crystal lattice. For silicates, the strongest bonds involve the siloxane (Si-O-Si) linkages. Consequently, the release rate of Si is controlled by the number of Si-O-Si bonds that have to be broken per Si atom, as shown for diopside²² (Figure 3 a). More generally, the silicate dissolution rate²³ complies with the periodic bond chain (PBC) theory²⁵, which states that crystal faces can be sorted according to the number of uninterrupted chains of energetically strong bonds (called PBCs) that they contain. The face dissolution rates

of a given crystal would therefore be related to the strength of these bonds, with the intrinsic reactivity negatively correlated with the number of PBCs per face.

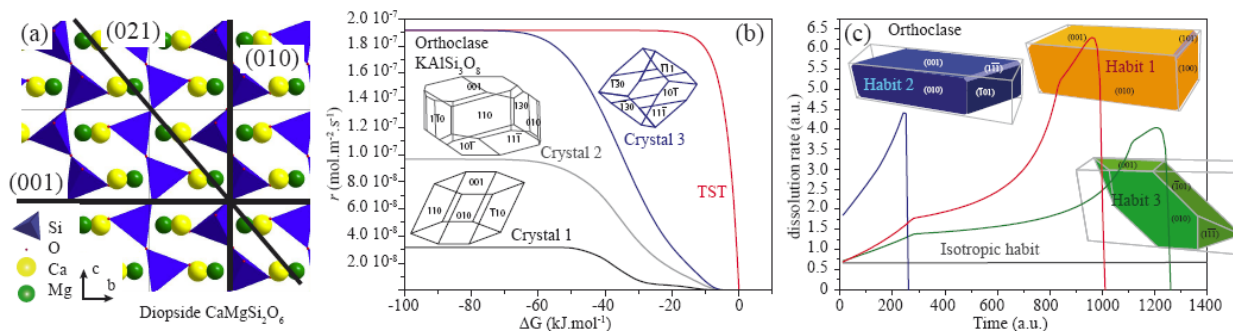


Figure 3. (a) Projection of diopside structure following [100] zone axis. The (001) and (021) faces intersect only one Si–O–Si bond per silicate tetrahedron, explaining their greater reactivity as opposed to (*hk0*) faces that intersect two Si–O–Si bonds²². (b) Modeled variation of orthoclase dissolution rate resulting from the temporal evolution of crystal morphology for various crystal habits²³. (c) Reconstruction of the rate- ΔG relationship for different orthoclase crystal habits, and comparison with the TST formulation²³.

2.4. Recognizing the dynamic nature of the surface area

Crystal growth and dissolution also show that the surface area is a dynamic parameter that evolves as the reaction progresses. The microtopography of pure micritic limestone fracture surface does not change very much during dissolution²⁶, whereas in polymineralic rocks, the increase in the total specific surface area is mostly due to the increase in the exposed surface of the less-reactive or non-reactive minerals^{26,27}. In that case, there is no correlation between surface roughness, geometric surface area (determined at a given scale), and the *effective* surface area.

An equally challenging aspect of the carbonation process resides in the proportion of the dissolving mineral surface area that is in contact with the fluid while heterogeneous nucleation and growth of new precipitates occur at the surface. Although an *effective* surface area evolution can be successfully proposed for the carbonation reaction to account for this effect²⁸, it basically has little to no predictive power, as it is often fitted *a posteriori*. The observation that mineral replacement reactions can still proceed while the apparent surface area of the primary minerals is virtually nil is even more problematic²⁹, emphasizing that fitting the surface area term for modeling perspectives is unlikely to provide reliable outputs.

2.5. Limitations of the conventional use of the surface area concept and perspectives

Regarding the abovementioned discussion, the definition of an overall isotropic and homogeneous “*effective*” surface area is confusing. In particular, the recognition of the anisotropic nature of mineral reactivity has far-reaching consequences with respect to the conventional treatment of kinetics. First, the rates obtained from bulk experiments on powders may not provide more than empirical relations because the apparent overall dissolution rates are intimately related to the morphologies of the individual grains. Second, the relationship between r_{min} and ΔG cannot be considered universal because it is also related to the crystal geometry (Figure 3b). Finally, the evolution of the crystal morphology as the dissolution progresses²³ (Figure 3c) challenges the paradigm of immutability and the definition of a unique rate constant for each mineral.

However, the anisotropic nature of mineral reactivity may not be detrimental to the modeling of CO₂-water-rock interactions, as some simplifications are conceivable. For instance, at the reservoir scale, most rocks have a fabric, i.e., a preferred arrangement and orientation of minerals. Therefore, fluid flow paths and mineral dissolution/precipitation rates may be

intimately related⁷, such that the rock reactivity might be better described based on the modeling of a limited number of crystal habits that are characteristic of the considered geological setting.

Referring back to the *effective* surface area concept¹², several studies have also shown that the *effective* surface area, for the most part, actually reflects--and therefore includes--the transport limitations near the interface as a result of the development of complex surface topography²⁶ or microporous network³⁰, the formation of microcoating³¹ or passivation^{28,32} by newly formed phases. More generally, the global reactivity results from a complex interplay between surface reaction kinetics and transport both near the fluid-mineral interface and throughout the porous network, i.e., along the flow paths.

3. COUPLED CHEMISTRY-GEOMETRY-TRANSPORT PROCESSES ACROSS SCALES

The question of coupling between chemical reactions and transport both in the vicinity of the fluid-solid interface and within a pore (Figure 4) is central to a better understanding of how spatially heterogeneous chemical fluxes spread over larger scales. At the pore scale, the equation for describing reactive transport in the fluid phase can be written:

$$\frac{\partial C_i}{\partial t} = -\nabla \cdot (\mathbf{u}C_i) + D_i \nabla^2 C_i + \sum_{j=1}^N \nu_{i,j} r_j^* \quad (4)$$

where C_i and D_i are the concentration and diffusion coefficient of species i , respectively; \mathbf{u} is the fluid velocity; and $\sum_{j=1}^N \nu_{i,j} r_j^*$ is the source/sink kinetic term, which accounts for homogeneous reactions in the fluid phase and heterogeneous reactions at the mineral surface.

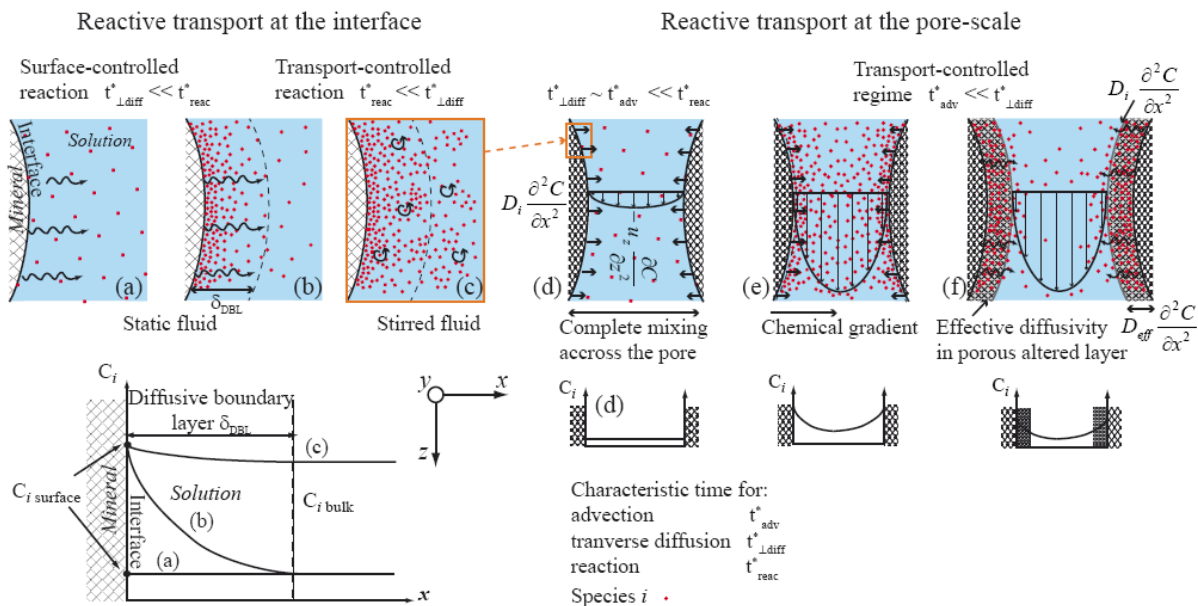


Figure 4. Schematic representation of the reactive transport phenomena both at the fluid-mineral interface and at the pore scale.

The different characteristic times for advective transport, transverse diffusion from/to the interface and chemical reactions at the mineral surface (which are related to the three right-end side terms of Eq.4, respectively) lead to either surface-controlled or transport-controlled conditions. When the dissolution/precipitation reaction is slow, the reaction is surface-controlled, and r_j^* is normally equal to the effective dissolution/precipitation rate, r_{min} , as defined by Eq.3. However, for large geochemical disequilibrium, the kinetic term can be so large that chemical reactions become transport-controlled at the interface to the extent of making concentration gradients appear in a diffusive boundary layer. In that case, the global flux of elements becomes highly dependent on the local flow regime in the immediate vicinity of the interface (Figure 4a-c).

However, regardless of the rate-limiting process at the fluid-solid interface, i.e. transport-controlled or surface-controlled, further mass-transport limitations between the mineral surface and the pore center (Figure 4d-f) can lead, at the pore scale, to poorly mixed conditions¹⁰. The heterogeneous pore structures also favor the development of chemical gradients, which induce a scale dependence of the mineral reaction rates at a larger scale³³, i.e., within the porous network, due to the heterogeneous distribution of fluid velocities.

Because the fluid velocity field is intimately related to the pore geometry, the changes in the microstructures of both minerals and rocks with time control this coupling and, ultimately, the reactivity at different levels. Applications of non-invasive XMT have permitted direct tracking of the evolution of the fluid-mineral interface during reactive flow within fractures or porous media^{5,27,34}. In monomineralic rocks, fluid penetration along grain boundaries and microcracks results in an increase in the accessibility of the reactive surface area exposed to the fluid³⁰. In that respect, the larger proportion of grain boundaries where dissolution proceeds in microcrystalline calcite may partly explain the order of magnitude difference in the dissolution rate compared to that of coarsely crystalline calcite²⁰. The presence of calcite crystals with different sizes and, therefore, different reactive surface areas leads to an increase in the surface roughness, thus disturbing the flow field in the vicinity of the fluid-rock interface. A microporous microscale network progressively develops as well, favoring the development of diffusive paths linked to the main flow paths. We have shown that the microcrystalline texture contributes to the enhancement of the reactivity of some limestones over time³⁰, which is in contrast to most experimental observations in that type of rock, where fluxes generally decrease or remain almost constant^{27,35,36}. Using trace elements, the reactivity of calcite was shown to also be grain-size dependent with different contributions over time from the two types of calcite. The empirical

sugar lump model³⁰ shows the difficulty of defining a reactive surface for mineral aggregates to model the changes in reactivity over time, echoing the limitations described in the previous section.

The reactivity of silicates is also highly sensitive to the microstructural modifications at the fluid/mineral interface. A common feature of silicate dissolution is the formation of nm- to μm -thick ASSLS (Figure 5a,b) resulting from the incongruent release of cations³⁷. The potential rate-controlling ability of ASSLS is implicitly based on the following fundamental question: can water freely reach the pristine silicate surface despite the development of ASSLS? ASSLS have long been considered to be leached layers resulting from the exchange between protons from the solution and labile cations from the mineral surface, followed by solid-state volume interdiffusion of protons with cations within the layer¹⁶. In this model, the difference in chemical potentials between the bulk solution and the passivating surface layer itself is considered to be the driving force of the reaction³⁸. However, recent studies support that ASSLS result from interfacial dissolution/precipitation processes, indirectly suggesting that water can actually circulate through ASSLS^{37,39}, restoring the difference in the chemical potentials between the solution and the bulk mineral as the driving force of the dissolution. Unravelling the transport properties through ASSLS is central to elucidating these conflicting models. Several studies^{28,32,40-42} have highlighted that ASSLS may be understood as a nanoporous medium whose diffusivity greatly depends on the chemical composition of both the aqueous solution and the dissolving mineral. In particular, Fe(III) plays a major role in ASSL passivation, possibly due to the strong affinity of Fe(III)-bearing nanocrystals for silica⁴¹. In olivine^{32,42}, for instance, the breakdown of the ASSL ultimately controls the dissolution/carbonation rate. Conversely, under

similar P_{CO_2} and temperature conditions, the dissolution/carbonation rate of Fe-free silicates, e.g., wollastonite, is poorly affected by the formation of ASSLs²⁹.

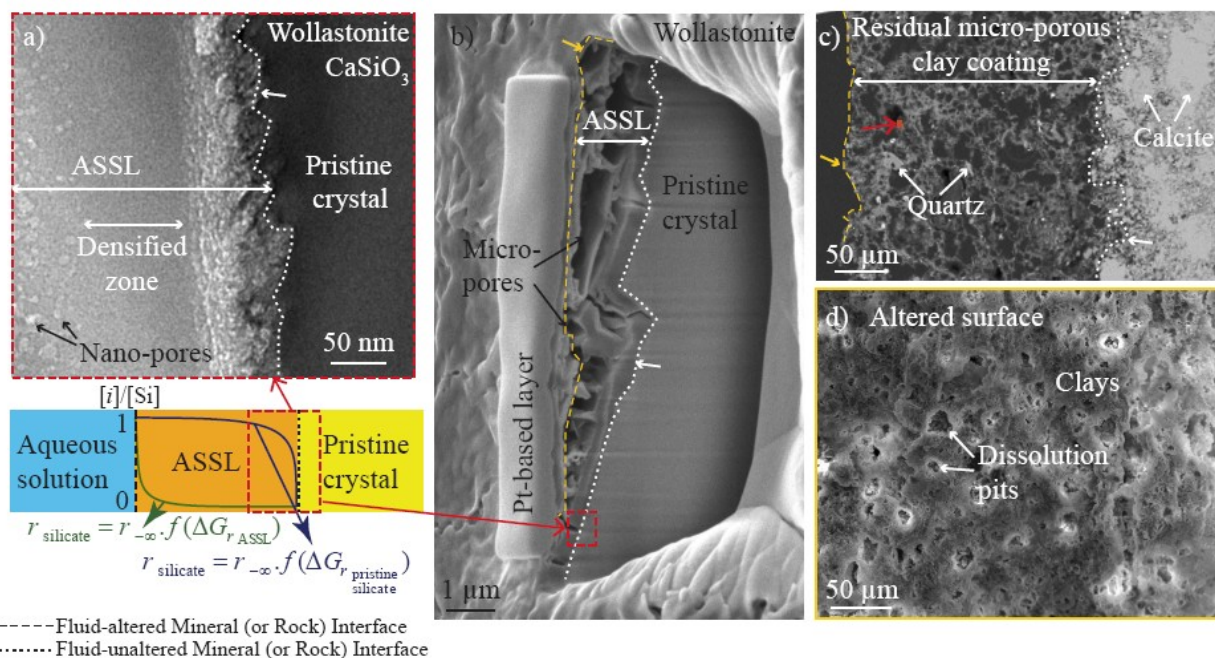


Figure 5. FIB-TEM observation (a) of the nanoporous ASSL-wollastonite interface after dissolution (see ^{28,30} for experimental details). Transport of reactant *i* through the ASSLs is controlled by its diffusivity (two extreme cases are schematically represented), which ultimately impacts the driving force of the reaction, and (b) evidence for micropores in the ASSLs. SEM observation of (c) a residual microporous clay coating in an argillaceous limestone fracture after dissolution (experimental conditions: $T = 22^\circ\text{C}$, $P_{\text{CO}_2} = 1 \text{ bar}$, $Q = 2 \text{ cm}^3 \cdot \text{hr}^{-1}$, $t = 168 \text{ hr}$) and (d) the altered fracture wall surface.

The exponential decrease of the chemical fluxes observed during the development of ASSLs in silicates has also been observed in rocks³¹ whose forming minerals have very different dissolution rates. In that case, the dissolution of calcite grains is associated with the development

of a residual microporous silicate coating near the fluid–mineral interface (Figure 5c,d), which results in a decrease in the transport efficiency by increasing the diffusion compared to the advection close to the surface of the reacting minerals (Figure 4). The growth of the alteration layer also results in an increase in the surface area of low-reactivity minerals exposed to the flowing fluid, increasing for instance the number of sites for adsorption on clays, which can also contribute to retardation of contaminants⁴³.

At a larger scale, reactive transport can result in the development of preferential flow paths in both monomineralic and polymineralic rocks, also leading to a global reduction of the chemical fluxes³⁵ (Figure 6a,b). Generally, the governing parameters for changing the pore space are related by the local Péclet ($Pe = u L^* / D$) and Damköhler ($Da = k_r' L^{*2} / D$) numbers⁸, where u is the fluid velocity, D is the molecular diffusion, k_r' is a first order kinetic constant [s^{-1}], and L^* is a characteristic length, e.g., the pore size. Pe and Da compare the advective transport properties of the flowing fluid and the chemical reactive properties of the solid matrix with molecular diffusion, respectively.

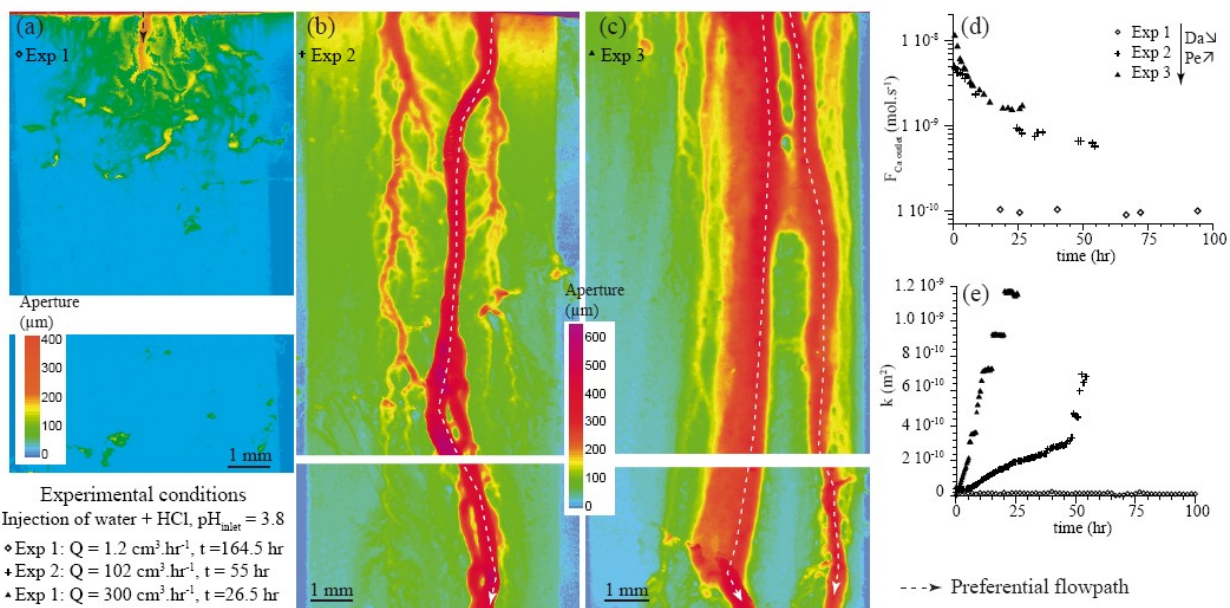


Figure 6. (a) Aperture maps derived from XMT datasets of artificial, initially parallel flat limestone fractures after reactive flow experiments at different Da and resulting (b) chemical fluxes and (c) permeability evolutions with time.

The fluid velocity and mineral reactivity play primary roles in determining under what regime the dissolution/precipitation reactions progress in porous media, from uniform propagation of front to the formation of localized flow paths or barriers. The highest reactivity zones are concentrated at the boundary where a large chemical disequilibrium is maintained or along preferential flow paths where fluid renewal is the fastest. The patterns are directly linked to reaction instabilities⁴⁴, as the reactive fluid infiltrates areas of higher permeability. For dissolution, a positive feedback between transport and chemical reactions develops, and leads to the growth of wormholes. For precipitation, a negative feedback develops. Precipitation is favored in the areas where the supersaturation is the highest, i.e., near the reaction front and in

the preferential flowpaths^{34,45} (Figure 7a). A precipitation barrier can even form, resulting in flow diversion, which may lead to the complete sealing of the reaction front.

However, Pe and Da only give a qualitative estimation of the extent of the mass transfer limitation at a given time and location (compared to the numerical resolution of Eq. 4) and should be taken with a pinch of salt⁶. Indeed, the progression of unstable fronts is also related to the initial pore space heterogeneities³⁶. In addition, the transient nature of reactive transport, while reaction kinetics varies over several orders of magnitude between far-from and close-to equilibrium and a progressive reorganization of flow occurs, confers non-steady natures on Da and Pe .

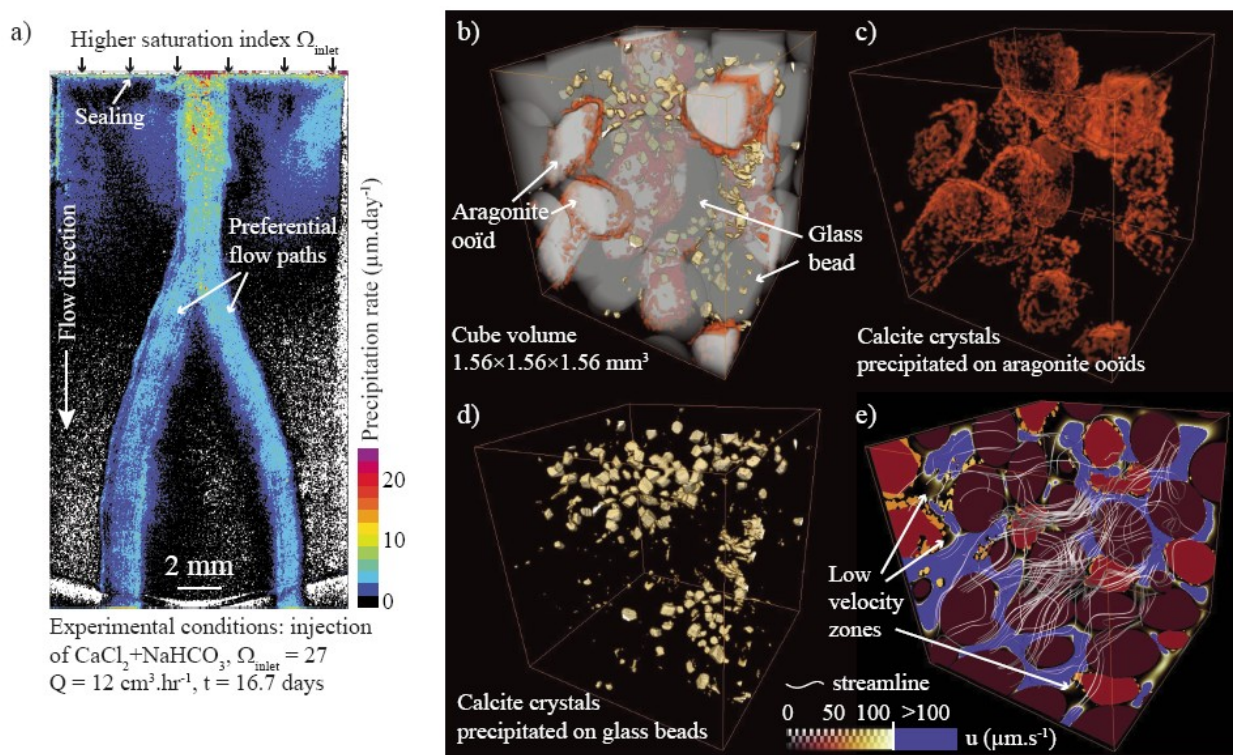


Figure 7. (a) Calcite precipitation rate distribution derived from XMT datasets in an artificial, flat and grooved dolomitic limestone fracture. (b-d) Precipitation patterns in porous analogue of sandstone and (e) resulting flow patterns (see⁴⁸ for experimental details).

4. POROSITY-PERMEABILITY EVOLUTION

Pore-scale feedbacks between geochemistry and flow drive the changes in permeability (Figure 6 c). Intuitively, carbonation should lead to a global reduction of permeability by globally decreasing the reservoir porosity. However, an increase in permeability due to dissolution is likely to occur near the injection well, whereas healing of the fluid paths by cementation of grain boundaries⁴⁶ is expected further in the reservoir. Crystallization pressure resulting from precipitation of carbonates or salts could also induce fracturing and creation of new flow paths⁴⁷.

The evolution of permeability depends on how the pore space is affected by reactions and is not solely a function of porosity changes. The reaction regime is a major controlling factor of the porosity-permeability relationship. While transport-limited dissolution reactions favor a rapid increase of permeability due to preferential widening of narrow pore throats where the fluid velocity is higher, surface-limited reactions should have a smaller impact due to a more homogeneous shift of the fluid-mineral interface⁵. For precipitation, the same reduction in porosity may lead to different reductions in permeability, as the preferential localization of precipitation along preferential flow paths and in areas where the fluid is more oversaturated also depends on Pe and Da ⁴⁵ (Figure 7a). We have also shown that non-uniform precipitation patterns emphasize the permeability decrease by increasing the pore roughness⁴⁸. Indeed, the density, morphology and growth rate of newly precipitated crystals can be very different in the same pore^{34,48}, despite similar chemistry and flow conditions (Figure 7b,c,d), as it depends on the substrate surface energy and spatial distribution of minerals and may be affected by the flow and transport conditions near the interface (Figure 7e).

In addition, detachment, solid transport and deposition of low-reactivity minerals contained in reacting matrix, e.g., clays, also deserve to be considered, as decreases in permeability and even clogging of the flow paths despite net dissolution have been reported^{31,49}.

All considered, the prediction of permeability evolution in reservoirs is somewhat challenging considering the number of factors that can affect the dynamics of flow path enlargement or clogging. In addition, the sample-size limitations of the high-resolution imaging techniques limit our ability to predict reliable porosity-permeability relationships at larger scales because permeability is a scale-dependent parameter.

5. CONCLUDING THOUGHTS

Pore-scale studies are revealing the complex natures of mineral reactivity and the interplay between chemistry, geometry, and flow and transport processes.

We have shown that the use of an effective surface area parameter is ambiguous. This concept may soon be superseded by physically more sound models that account for the observed rate distributions across reactive sites and crystal faces, such as emergent kinetic Monte Carlo (kMC) simulations based on bond-breaking probabilities^{3,50}, for which the limitations in terms of length scale could be overcome by combining kMC and Voronoï algorithms³.

In addition, continuum-scale geochemical modeling in porous media mostly relies on the fact that aqueous species can freely diffuse to and from pristine mineral surfaces, a condition that is not systematically met during the development of passivating ASSLs³² or microporous altered layers³¹, or the growth of newly precipitated crystals²⁸. Understanding the molecular mechanisms that govern the chemical fluxes in these layers and in the vicinity of the interface therefore likely represents a major challenge that must be overcome in the upcoming years to properly evaluate

carbonation rates. As water loses its bulk-like properties in pores narrower than 2 nm, further experimental and theoretical works will be required to evaluate the effective diffusivity in ASSLS, using either tracer percolation experiments coupled to nm-scale monitoring of the tracer penetration or molecular dynamics simulations⁵¹. Regardless of the scale, the dynamics of these growing layers, including repolymerization processes and morphological transformations^{31,52}, should also be investigated, as they ultimately govern the transport properties.

Conversely, heterogeneous pore structures combined with far-from-equilibrium conditions promote flow localization, and lead to reactivity enhancement in the preferential flow paths and unexpected changes in permeability, despite a global apparent decrease of reactivity.

Most importantly, these processes, which either enhance or decrease the reactivity, are not currently captured by large-scale modeling of reactive transport, albeit some continuum models are trying to capture the effect of micro-porous rates⁵³. Considering these new frontiers at interfaces, we suggest that upcoming works should focus on a better understanding of how the typical rock mineralogical composition and texture can impact the global reactivity of reservoirs injected with CO₂.

FIGURES

AUTHOR INFORMATION

Corresponding Author

*e-mail:catherine.noiriel@univ-tlse3.fr

Biographies

Catherine Noiriél grew up in Ramecourt, plain of Vosges. She earned a PhD in hydrogeology from Ecole de Mines de Paris in 2005. She is a lecturer at University Paul Sabatier in Toulouse. Her research focuses on low-temperature geochemistry and hydro-mechano-geochemical coupled processes at the pore scale.

Damien Daval was born in Vesoul, Haute-Saône. He received a PhD in geochemistry from Paris Diderot University in 2009. After a two-year fellowship at Lawrence Berkeley Lab, he joined the University of Strasbourg as a CNRS research scientist. His research focuses on the links between the microstructural modifications of the surface of dissolving geomaterials and their aqueous reactivity.

ACKNOWLEDGMENTS

C.N. thanks the Institute Carnot ISIFOR through the project SEQFRAC-450043 for supporting the preparation of this manuscript. Marion Pollet-Villard is acknowledged for providing raw material for the preparation of some of the figures. We also acknowledge the comments and suggestions made by the three anonymous reviewers, which were helpful to improve the manuscript.

REFERENCES

1. Kampman, N.; Bickle, M.; Wigley, M.; Dubacq, B., Fluid flow and CO₂-fluid-mineral interactions during CO₂-storage in sedimentary basins. *Chem. Geol.* **2014**, *369*, 22-50.
2. Loring, J. S.; Chen, J.; Benezeth, P.; Qafoku, O.; Ilton, E. S.; Washton, N. M.; Thompson, C. J.; Martin, P. F.; McGrail, B. P.; Rosso, K. M.; Felmy, A. R.; Schaef, H. T., Evidence for Carbonate Surface Complexation during Forsterite Carbonation in Wet Supercritical Carbon Dioxide. *Langmuir* **2015**, *31* (27), 7533-7543.

3. Fischer, C.; Luttge, A., Beyond the conventional understanding of water–rock reactivity. *Earth Planet. Sci. Lett.* **2017**, *457*, 100-105.
4. Pollet-Villard, M.; Daval, D.; Fritz, B.; Knauss, K. G.; Schäfer, G.; Ackerer, P., Influence of etch pit development on the surface area and dissolution kinetics of the orthoclase (001) surface. *Chem. Geol.* **2016**, *442*, 148-159.
5. Noiriél, C.; Bernard, D.; Gouze, P.; Thibaut, X., Hydraulic properties and microgeometry evolution in the course of limestone dissolution by CO₂-enriched water. *Oil & Gas Science and Technology* **2005**, *60* (1), 177-192.
6. Noiriél, C., Resolving time-dependent evolution of pore scale structure, permeability and reactivity using X-ray microtomography. *Rev. Mineral. Geoch.* **2015**, *80*, 247-286.
7. Peuble, S.; Andreani, M.; Godard, M.; Gouze, P.; Barou, F.; Van de Moortele, B.; Mainprice, D.; Reynard, B., Carbonate mineralization in percolated olivine aggregates: Linking effects of crystallographic orientation and fluid flow. *Am. Miner.* **2015**, *100* (2-3), 474-482.
8. Steefel, C. I.; Molins, S.; Trebotich, D., Pore scale processes associated with subsurface CO₂ injection and sequestration. *Rev. Mineral. Geoch.*, **2013**, *77*, 259-303.
9. Kaszuba, J.; Yardley, B.; Andreani, M., Experimental perspectives of mineral dissolution and precipitation due to carbon dioxide-water-rock interactions. *Rev. Mineral. Geoch.* **2013**, *77*, 153-188.
10. Molins, S., Reactive interfaces in direct numerical simulation of pore scale processes. *Rev. Mineral. Geoch.* **2015**, *80* 461-481.
11. Eyring, H., The activated complex and the absolute rate of chemical reactions. *Chem. Rev.* **1935**, *17*, 65-82.
12. Aagaard, P.; Helgeson, H. C., Thermodynamic and kinetic constrains on reaction-rates among minerals and aqueous solutions 1. Theoretical considerations. *Am. J. Sci.* **1982**, *282* (3), 237-285.
13. Brunauer, S.; Emmet, P. H.; Teller, E. A., Adsorption of gases in multimolecular layers. *J. Am. Chem. Soc.* **1938**, *60*, 309-319.
14. Gilman, J. J.; Johnston, W. G.; Sears, G. W., Dislocation Etch Pit Formation in Lithium Fluoride. *J. Appl. Phys.* **1958**, *29* (5), 747-754.
15. Lasaga, A. C.; Blum, A. E., Surface chemistry, etch pits and mineral-water reactions. *Geochim. Cosmochim. Acta* **1986**, *50* (10), 2363-2379.
16. Schott, J.; Pokrovsky, O. S.; Oelkers, E. H., The Link Between Mineral Dissolution/Precipitation Kinetics and Solution Chemistry. *Thermodynamics and Kinetics of Water-Rock Interaction* **2009**, *70*, 207-258.
17. Schott, J.; Brantley, S. L.; Drear, D.; Guy, C.; Borcsik, M.; Willaime, C., Dissolution kinetics of strained calcite. *Geochim. Cosmochim. Acta* **1989**, *53*, 373-382.
18. Lasaga, A. C.; Luttge, A., Variation of Crystal Dissolution Rate Based on a Dissolution Stepwave Model. *Science* **2001**, *291*, 2400-2404.
19. Smith, M. E.; Knauss, K. G.; Higgins, S. R., Effects of crystal orientation on the dissolution of calcite by chemical and microscopic analysis. *Chem. Geol.* **2013**, *360*, 10-21.
20. Fischer, C.; Arvidson, R. S.; Lüttge, A., How predictable are dissolution rates of crystalline material? *Geochim. Cosmochim. Acta* **2012**, *98*, 177-185.
21. Arvidson, R. S.; Beig, M. S.; Lüttge, A., Single-crystal plagioclase feldspar dissolution rates measured by vertical scanning interferometry. *Am. Miner.* **2004**, *89* (1), 51-56.

22. Daval, D.; Hellmann, R.; Saldi, G. D.; Wirth, R.; Knauss, K. G., Linking nm-scale measurements of the anisotropy of silicate surface reactivity to macroscopic dissolution rate laws: New insights based on diopside. *Geochim. Cosmochim. Acta* **2013**, *107* (0), 121-134.
23. Pollet-Villard, M.; Daval, D.; Ackerer, P.; Saldi, G. D.; Wild, B.; Knauss, K. G.; Fritz, B., Does crystallographic anisotropy prevent the conventional treatment of aqueous mineral reactivity? A case study based on K-feldspar dissolution kinetics. *Geochim. Cosmochim. Acta* **2016**, *190*, 294-308.
24. King, H. E.; Satoh, H.; Tsukamoto, K.; Putnis, A., Surface-specific measurements of olivine dissolution by phase-shift interferometry. *Am. Miner.* **2014**, *99* (2-3), 377-386.
25. Hartman, P.; Perdok, W. G., On the relations between structure and morphology of crystals. I. *Acta Crystallogr.* **1955**, *8* (1), 49-52.
26. Gouze, P.; Noiriél, C.; Bruderer, C.; Loggia, D.; Leprovost, R., X-Ray tomography characterisation of fracture surfaces during dissolution. *Geophys. Res. Lett* **2003**, *30* (5), 1267, doi:10.1029/2002/GL016755.
27. Noiriél, C.; Gouze, P.; Made, B., 3D analysis of geometry and flow changes in a limestone fracture during dissolution. *Journal of Hydrology* **2013**, *486*, 211-223.
28. Daval, D.; Martinez, I.; Corvisier, J.; Findling, N.; Goffe, B.; Guyot, F., Carbonation of Ca-bearing silicates, the case of wollastonite: Experimental investigations and kinetic modeling. *Chem. Geol.* **2009**, *265* (1-2), 63-78.
29. Putnis, A., Mineral Replacement Reactions. *Thermodynamics and Kinetics of Water-Rock Interaction* **2009**, *70*, 87-124.
30. Noiriél, C.; Luquot, L.; Madé, B.; Raimbault, L.; Gouze, P.; van der Lee, J., Changes in reactive surface area during limestone dissolution: An experimental and modelling study. *Chem. Geol.* **2009**, *265* (1-2), 160-170.
31. Noiriél, C.; Madé, B.; Gouze, P., Impact of coating development on the hydraulic and transport properties in argillaceous limestone fracture. *Water Resour. Res.* **2007**, *43*, W09046, doi:10.1029/2006WR005379.
32. Daval, D.; Sissmann, O.; Menguy, N.; Saldi, G. D.; Guyot, F.; Martinez, I.; Corvisier, J.; Garcia, B.; Machouk, I.; Knauss, K. G.; Hellmann, R., Influence of amorphous silica layer formation on the dissolution rate of olivine at 90 degrees C and elevated pCO₂. *Chem. Geol.* **2011**, *284* (1-2), 193-209.
33. Li, L.; Peters, C. A.; Celia, M. A., Effects of mineral spatial distribution on reaction rates in porous media. *Water Resour. Res.* **2007**, *43* (1), doi10.1029/2005WR004848.
34. Noiriél, C.; Steefel, C. I.; Yang, L.; Ajo-Franklin, J., Upscaling calcium carbonate precipitation rates from pore to continuum scale. *Chem. Geol.* **2012**, *318-319*, 60-74.
35. Luquot, L.; Gouze, P., Experimental determination of porosity and permeability changes induced by injection of CO₂ into carbonate rocks. *Chem. Geol.* **2009**, *265* (1-2), 148-159.
36. Smith, M. M.; Sholokhova, Y.; Hao, Y.; Carroll, S. A., CO₂-induced dissolution of low permeability carbonates. Part I: Characterization and experiments. *Adv. Water Resour.* **2013**, *62*, 370-387.
37. Hellmann, R.; Wirth, R.; Daval, D.; Barnes, J.-P.; Penisson, J.-M.; Tisserand, D.; Epicier, T.; Florin, B.; Hervig, R. L., Unifying natural and laboratory chemical weathering with interfacial dissolution–reprecipitation: A study based on the nanometer-scale chemistry of fluid–silicate interfaces. *Chem. Geol.* **2012**, *294–295* (0), 203-216.
38. Oelkers, E. H., General kinetic description of multioxide silicate mineral and glass dissolution. *Geochim. Cosmochim. Acta* **2001**, *65* (21), 3703-3719.

39. Ruiz-Agudo, E.; King, H. E.; Patino-Lopez, L. D.; Putnis, C. V.; Geisler, T.; Rodriguez-Navarro, C.; Putnis, A., Control of silicate weathering by interface-coupled dissolution-precipitation processes at the mineral-solution interface. *Geology* **2016**, *44* (7), 567-570.
40. Saldi, G. D.; Daval, D.; Guo, H.; Guyot, F.; Bernard, S.; Le Guillou, C.; Davis, J. A.; Knauss, K. G., Mineralogical evolution of Fe–Si-rich layers at the olivine-water interface during carbonation reactions. *Am. Miner.* **2015**, *100* (11-12), 2655-2669.
41. Saldi, G. D.; Daval, D.; Guo, H.; Guyot, F.; Bernard, S.; Le Guillou, C.; Davis, J. A.; Knauss, K. G., Mineralogical evolution of Fe–Si-rich layers at the olivine-water interface during carbonation reactions. *Am. Miner.* **2015**, *100* (11-12), 2655-2669.
42. Maher, K.; Johnson, N. C.; Jackson, A.; Lammers, L. N.; Torchinsky, A. B.; Weaver, K. L.; Bird, D. K.; Brown Jr, G. E., A spatially resolved surface kinetic model for forsterite dissolution. *Geochim. Cosmochim. Acta* **2016**, *174*, 313-334.
43. Tournassat, C.; Steefel, C. I., Ionic Transport in Nano-Porous Clays with Consideration of Electrostatic Effects. *Rev. Mineral. Geoch.*, **2015**, *80*, 287-329.
44. Ortoleva, P. J.; Chadam, J.; Merino, E.; Sen, A., Geochemical self-organization II. The reactive infiltration instability. *Am. J. Sci.* **1987**, *287*, 1008-1040.
45. Tartakovsky, A. M.; Meakin, P.; Scheibe, T. D.; Wood, B. D. C. W., A smoothed particle hydrodynamics model for reactive transport and mineral precipitation in porous and fractured porous media. *Water Resour. Res.* **2007**, *43* (5).
46. Hövelmann, J.; Austrheim, H.; Jamtveit, B., Microstructure and porosity evolution during experimental carbonation of a natural peridotite. *Chem. Geol.* **2012**, *334* (0), 254-265.
47. Zhu, W.; Fousseis, F.; Lisabeth, H.; Xing, T.; Xiao, X.; De Andrade, V.; Karato, S.-i., Experimental evidence of reaction-induced fracturing during olivine carbonation. *Geophys. Res. Lett* **2016**, *43* (18), 9535-9543.
48. Noiriél, C.; Steefel, C. I.; Yang, L.; Bernard, D., Effects of pore-scale heterogeneous precipitation on permeability and flow *Adv. Water Resour.* **2016**, *95*, 125-137.
49. Mangane, P. O.; Gouze, P.; Luquot, L., Permeability impairment of a limestone reservoir triggered by heterogeneous dissolution and particles migration during CO₂-rich injection. *Geophys. Res. Lett* **2013**, *40* (17), 4614-4619.
50. Kurganskaya, I.; Lutge, A., A comprehensive stochastic model of phyllosilicate dissolution: Structure and kinematics of etch pits formed on muscovite basal face. *Geochim. Cosmochim. Acta* **2013**, *120* (0), 545-560.
51. Bourg, I. C.; Steefel, C. I., Molecular Dynamics Simulations of Water Structure and Diffusion in Silica Nanopores. *J. Phys. Chem. C* **2012**, *116* (21), 11556-11564.
52. Cailleateau, C.; Angeli, F.; Devreux, F.; Gin, S.; Jestin, J.; Jollivet, P.; Spalla, O., Insight into silicate-glass corrosion mechanisms. *Nat. Mater.* **2008**, *7* (12), 978-983.
53. Deng, H.; Molins, S.; Steefel, C.; DePaolo, D.; Voltolini, M.; Yang, L.; Ajo-Franklin, J., A 2.5D Reactive Transport Model for Fracture Alteration Simulation. *Environ. Sci. Technol.* **2016**, *50* (14), 7564-7571.